Combination of FT-ICR mass spectrometry and spectroscopy for the characterization of ion structures

Guillaume van der Rest
Institut de Chimie Physique
Université Paris-Saclay

Outline

1. Advantages and limitations of FT-ICR cells for ion spectroscopy
2. Single photon processes
3. Multiple photon processes

WHY USE FT-ICR FOR ION PHOTODISSOCIATION ?

Ion storage in ICR cells

Dates back to before FT was introduced.

Photodissociation of the CH_3Cl^+ and N_2O^+ Cations

Robert C. Dunbar*

Contribution from the Department of Chemistry, Stanford University, Stanford, California 94305. *Received October 2, 1970*

Abstract: The ion cyclotron resonance technique was used to observe the photodissociation of the cations CH_3Cl^+ and N_2O^+ in the gas phase. Ions were trapped in the icr cell for periods of the order of seconds, which permitted the photodissociation process to be observed with wavelength-selected light. A cyclotron resonance ejection technique was employed to show that CH_3Cl^+ ions were being dissociated rather than the CH_3ClH^+ ions which were also present. The photodissociation cross section for N_2O^+ was found to be roughly 0.25×10^{-18} cm² without strong wavelength dependence between 4000 and 6500 Å. The cross section for CH_3Cl^+ showed a large peak at 3150 Å, having a value at that wavelength of 7.8×10^{-18} cm². Possible assignments of this peak are considered, and it is suggested that photodissociation occurs through an ion excitation involving a change in occupation of the bonding or antibonding orbitals of the C–Cl bond.

R.C. Dunbar, J. Am. Chem. Soc. **93**, 4354 (1971)

Ion storage in ICR cells

At low field, FT-ICR allowed **long storage times** for the ions.

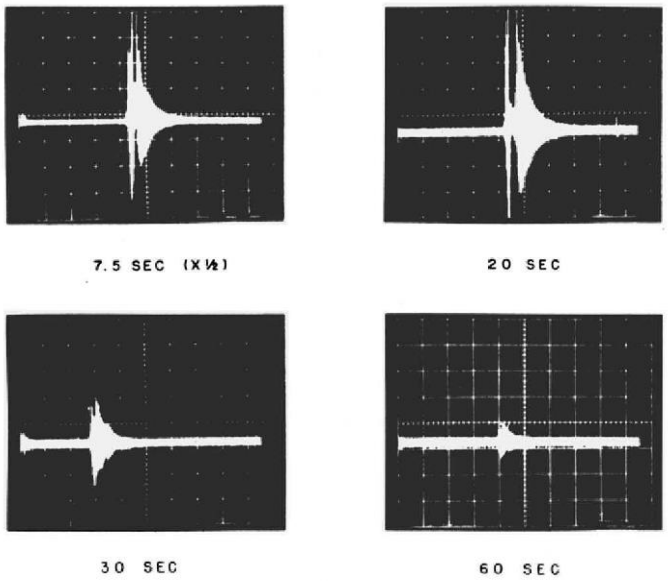

Figure 2. Ion trapping. The trapping of H_3O^+ ions under conditions of extremely long trapping is shown. The traces shown indicate a trapping time of about 30 sec for H_3O^+.

Wavelength tunability allows recording of an **action spectrum** of the CH_3Cl^+ ion.

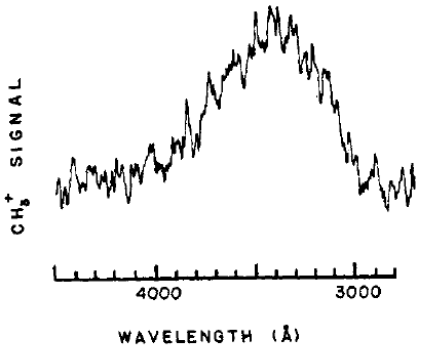

Figure 1. Production of CH_3^+ by photodissociation of CH_3Cl^+. The concentration of CH_3^+ in the icr cell is continuously monitored while the wavelength of the irradiating light from the monochromator is swept. The wavelength resolution (FWHM of the irradiating light) is 140 Å.

Ion beam and irradiation overlap

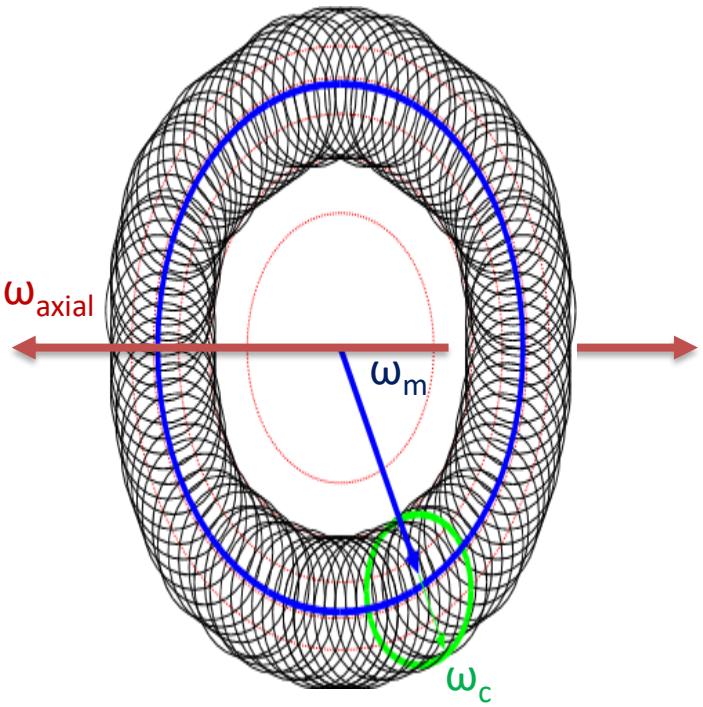

- Radiation needs to intersect the ion trajectory both in space and in time.
- Irradiation along the cell axis is the most usual setup.

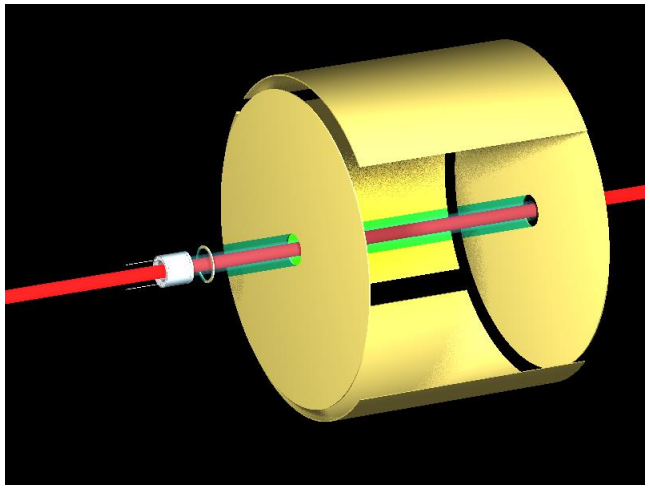

Ion beam and irradiation overlap

- On permanent magnet based instrument, irradiation can also be performed orthogonaly to the magnetic field.

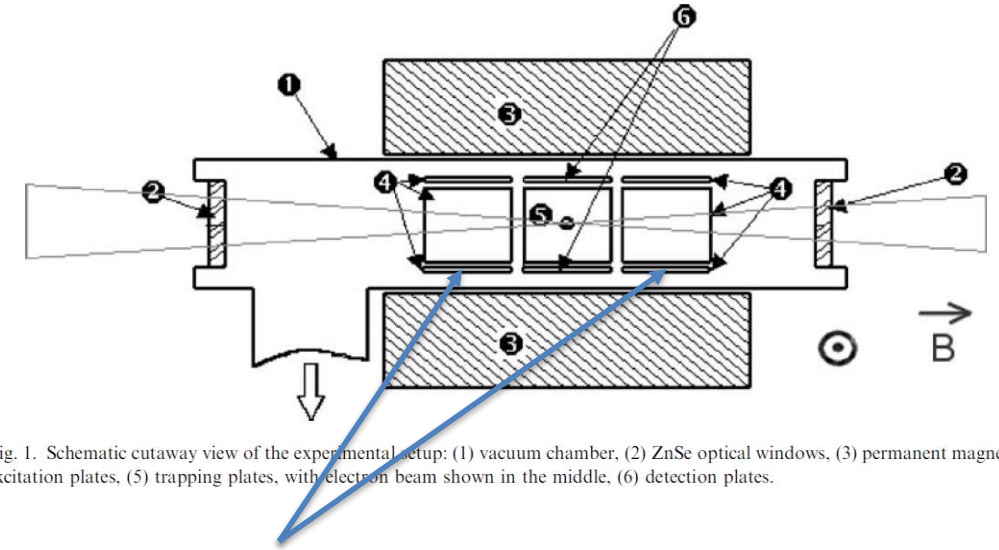

Fig. 1. Schematic cutaway view of the experimental setup: (1) vacuum chamber, (2) ZnSe optical windows, (3) permanent magnet, (4) excitation plates, (5) trapping plates, with electron beam shown in the middle, (6) detection plates.

Open ended excitation electrodes

*P. Maître et al. Nucl. Instrum. and Meth. Phys. Res. A **507** 541 (2003)*

Ion beam and irradiation overlap

- Issues with overlapping beams :
  - Highest power densities are achieved with tightly focused pulsed photon sources
  - FT-ICR is not optimal for this :
    - Axial motion is generally on the order of centimeters : requires very good on axis alignement of the light beam in order to cover the complete cloud.
    - Radial (magnetron / cyclotron) motions radius depends on the magnetic field, initial ion velocities but also alignment and centering of the cell axis and ion injection path. Order of magnitude: millimiter.
    - 3D ion traps perform much better (overall volume on the order of 1 mm^3)
  - Solutions :
    - Higher irradiation power with an unfocused beam (use of beam expanders in IRMPD for instance)
    - **(Pseudo) Continuous irradiation** : increase the irradiation time to average over ion positions (but beware that some ions might remain out of the beam).
    - **Pulsed irradiation :** timing and delay effects might dramatically change the results with a focused beam as the ion cloud sample will change over time.

Action spectrscopy vs absorption spectroscopy

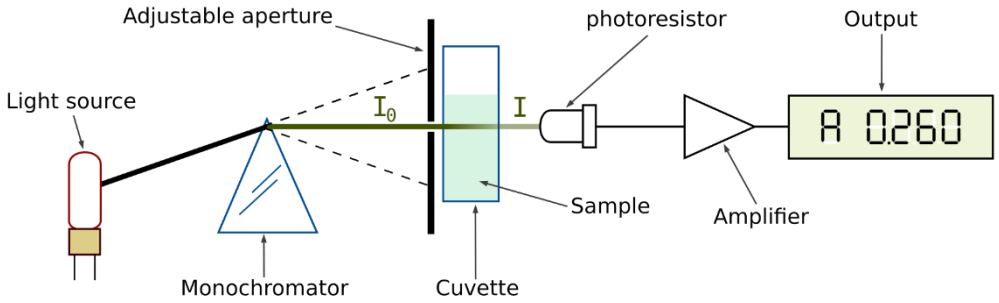

Standard spectrophotometer setup (source wikipedia)

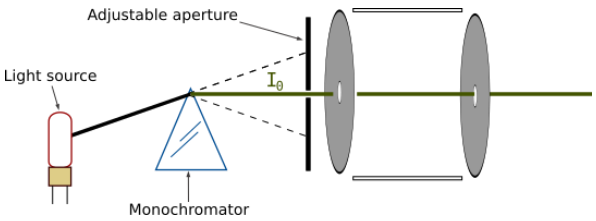

$$Eff = \frac{I_{frag}}{I_{prec} + I_{frag}}$$

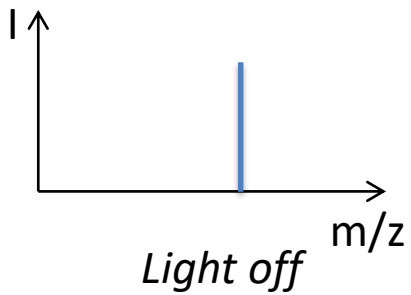

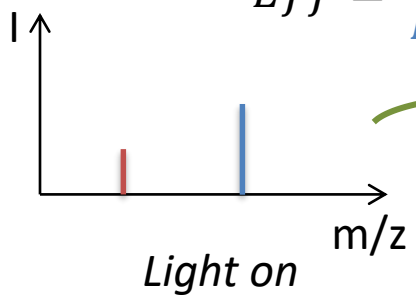

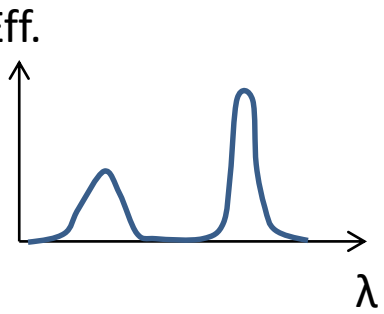

Pros and cons of FT-ICR vs ion traps for spectroscopy

- Cons :
  - Ion cloud overlap is more difficult to achieve compared to a 3D ion trap.
- Pros :
  - High resolution which can be achieved in the detection of product ions
  - Low pressure of the gas background : reduced thermalization effects.
    - Action spectroscopy assumes that absorption of a photon is related to fragmentation efficiency.

k_{-1} is composed of a collisional and a radiative component. Minimization of the collisional component improves the result.
This is even more the case for multiple photon processes.

SINGLE PHOTON PROCESSES

Photon activation (UV – Visible)

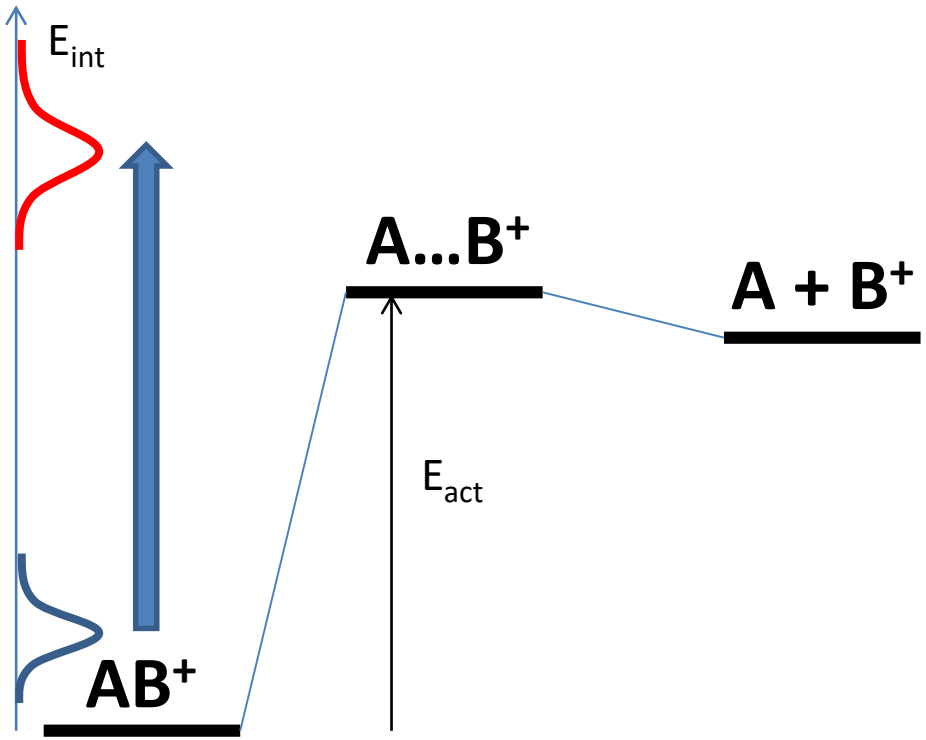

Single photon activation :

- Requires a photon with sufficient energy : ~ eV
- Requires an absorption band

- Proceeds through an electronic excited state, which can either directly dissociate or redistribute energy through intersystem crossing.

Tunable UV and FT-ICR

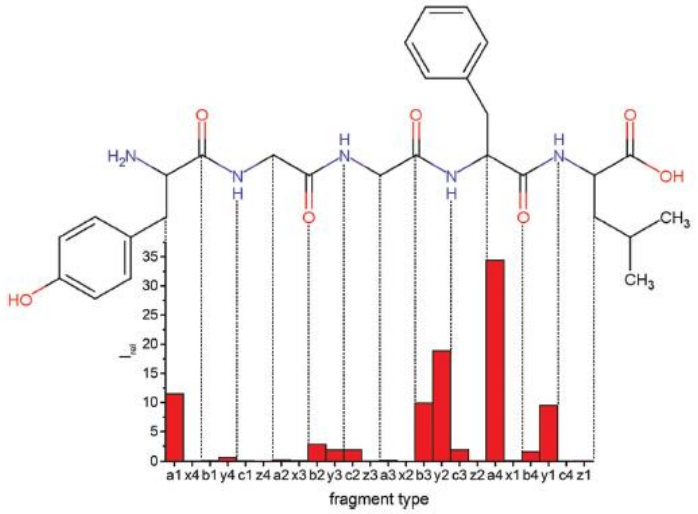

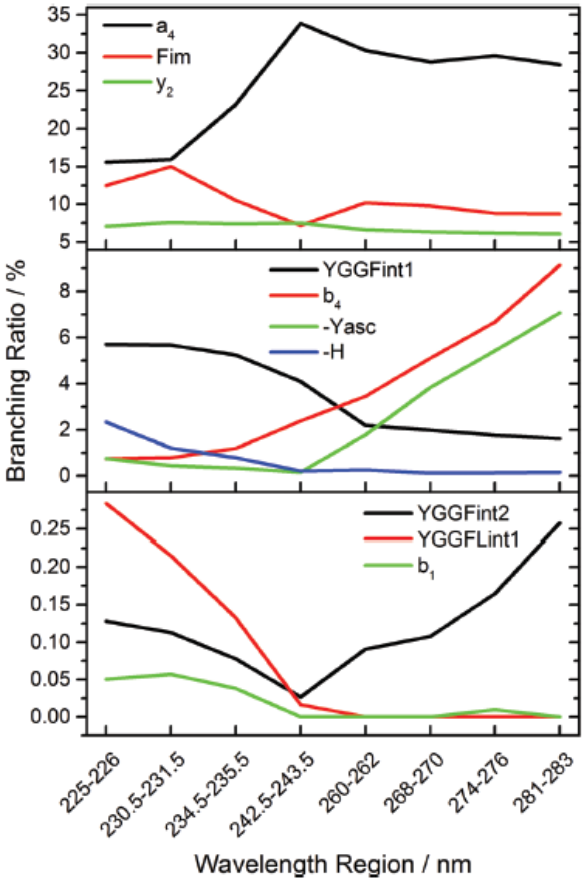

- Fragmentation favored close to the aromatic residues.
- Some dependence of the pathways on the laser wavelength.

A. Herburger, C. van der Linde, M. Beyer, Phys. Chem. Chem. Phys. **19** 10786 (2017)

Tunable UV-PD

- FT-ICR trap is quite ideal for alignment with a laser and long activation periods due to a low photon flux.

Validation on small systems: flavin co-factors of flavoproteins

OPO UV-Vis laser @ Ecole Polytechnique

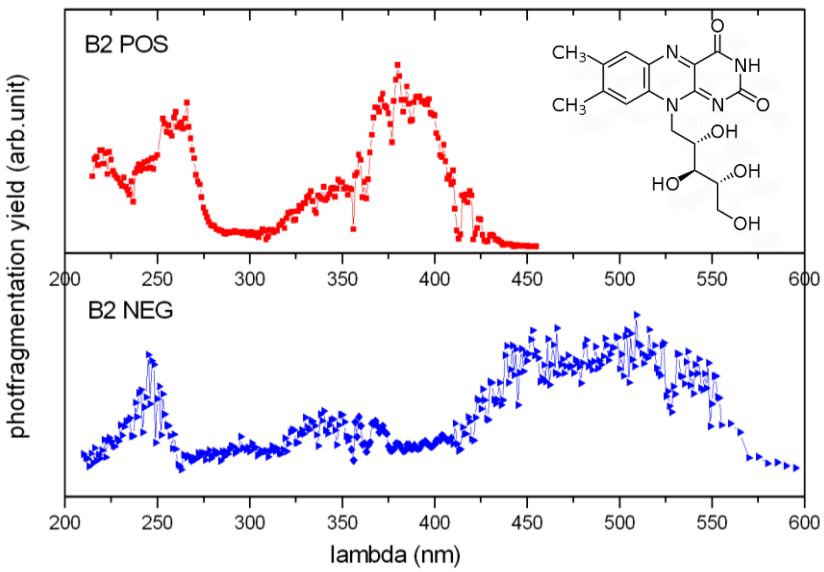

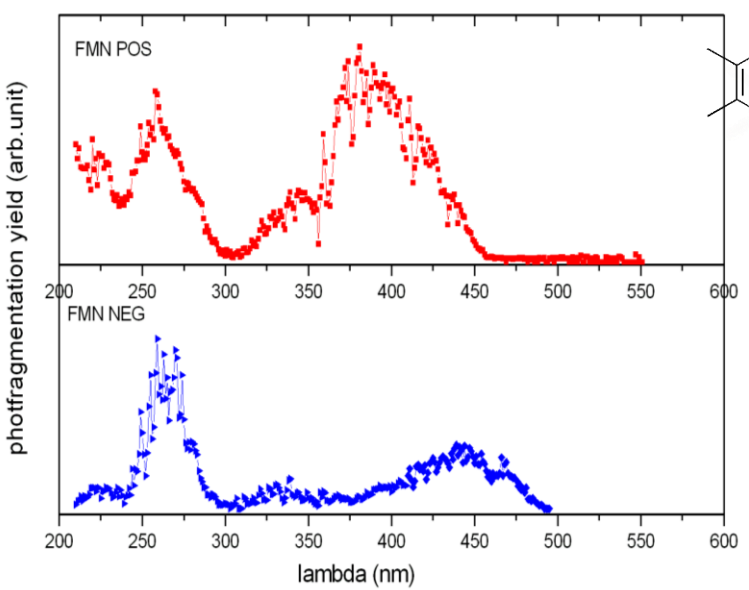

The optical response depends on the **chemical environment**

The optical response depends on the **charge environment**

UVPD at 213 nm

The Ups and Downs of Repeated Cleavage and Internal Fragment Production in Top-Down Proteomics

Yana A. Lyon,[1] Dylan Riggs,[1] Luca Fornelli,[2] Philip D. Compton,[2] Ryan R. Julian[1]

[1]Department of Chemistry, University of California, Riverside, 501 Big Springs Road, Riverside, CA 92521, USA
[2]Departments of Chemistry and Molecular Biosciences, and the Proteomics Center of Excellence, Northwestern University, N. Sheridan Road, Evanston, IL 60208, USA

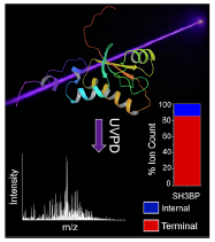

Abstract. Analysis of whole proteins by mass spectrometry, or top-down proteomics, has several advantages over methods relying on proteolysis. For example, proteoforms can be unambiguously identified and examined. However, from a gas-phase ion-chemistry perspective, proteins are enormous molecules that present novel challenges relative to peptide analysis. Herein, the statistics of cleaving the peptide backbone multiple times are examined to evaluate the inherent propensity for generating internal versus terminal ions. The raw statistics reveal an inherent bias favoring production of terminal ions, which holds true regardless of protein size. Importantly, even if the full suite of internal ions is generated by statistical dissociation, terminal ions are predicted to account for at least 50% of the total ion current, regardless of protein size, if there are three backbone dissociations or fewer. Top-down analysis should therefore be a viable approach for examining proteins of significant size. Comparison of the purely statistical analysis with actual top-down data derived from ultraviolet photodissociation (UVPD) and higher-energy collisional dissociation (HCD) reveals that terminal ions account for much of the total ion current in both experiments. Terminal ion production is more favored in UVPD relative to HCD, which is likely due to differences in the mechanisms controlling fragmentation. Importantly, internal ions are not found to dominate from either the theoretical or experimental point of view.
Keywords: UVPD, HCD, Statistical analysis, Internal ion

- Nd-YAG 5th harmonic
- Commercial device by Thermo
- Applied for top-down proteomics on Orbitrap systems

Femto-second laser induced dissociation

Technique introduced by G.E. Reid in 2009 for peptide fragmentation analysis, using an activation in a rf ion trap device.

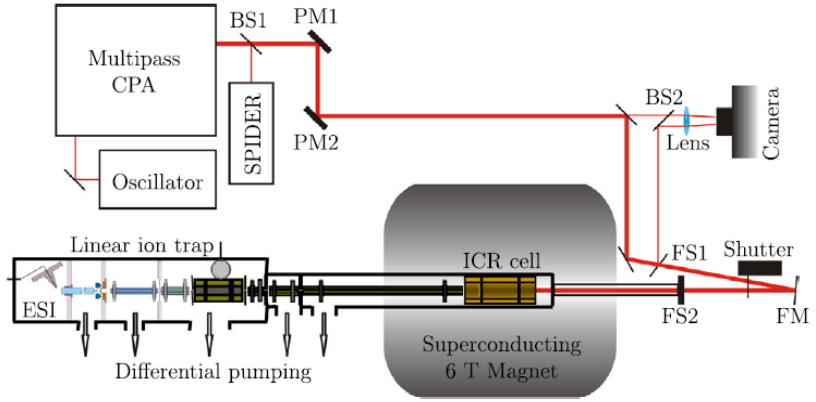

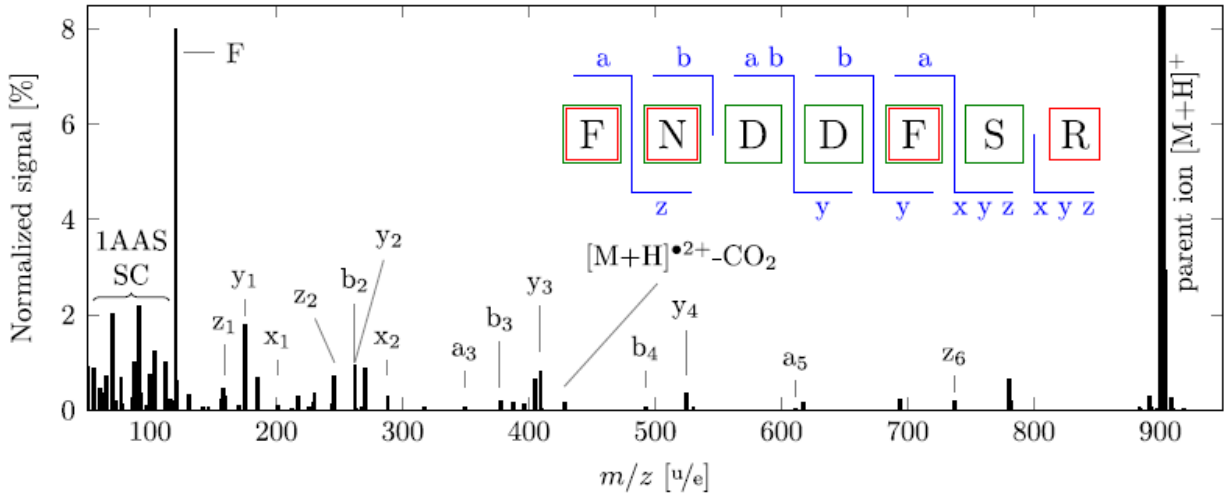

C. Neidel et al. Chem. Phys. (2018)

MULTIPLE PHOTON PROCESSES

Infra-red Multiphoton dissociation

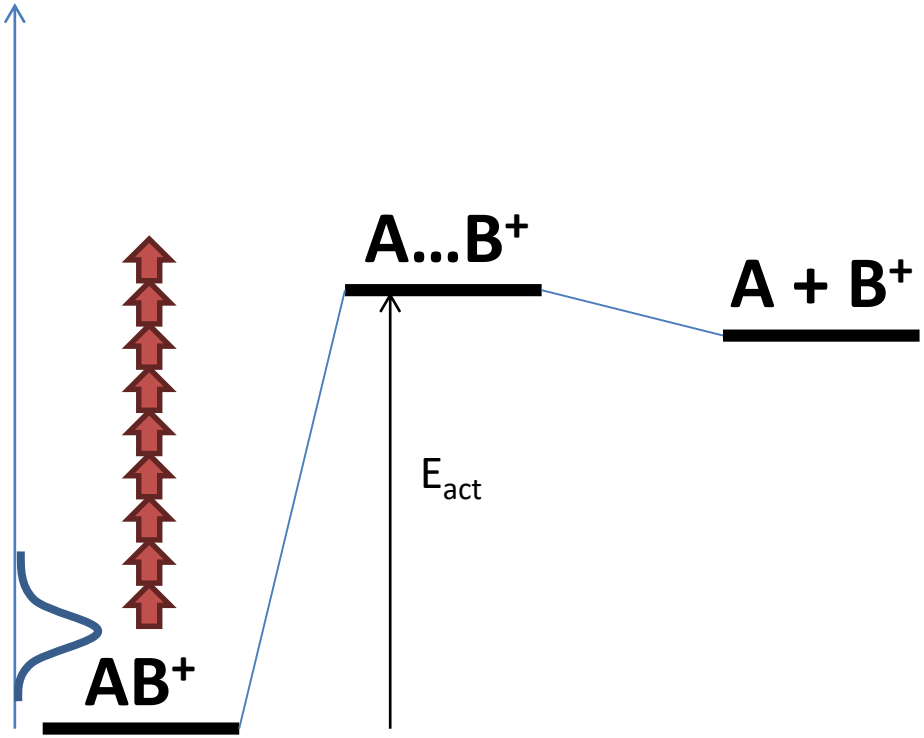

Multiple photon activation:

- IR photon ~ 0,1 eV
- Absorption of a number of photons is required to lead to fragmentation ***I**nfra-**R**ed **M**ulti-**P**hoton **D**issociation (IRMPD)*

- As for UVPD, an absorption band is required to observe fragmentation.

Wavelength ranges in IR spectroscopy

O-H / N-H stretches
Influenced by H-bonding

C-H stretches

Fingerprint region

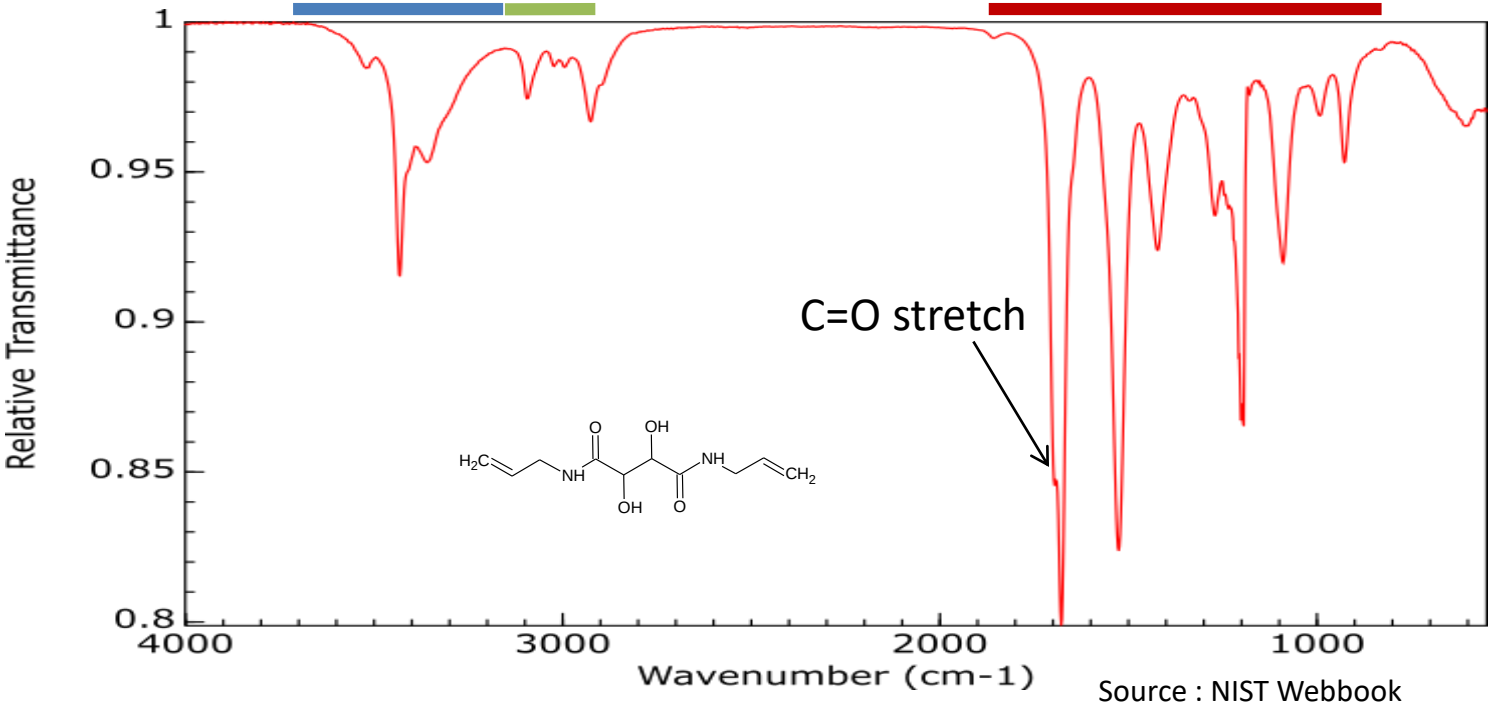

Source : NIST Webbook

Photon sources for IRMPD

- Tunable lasers – Free Electron lasers

Based on an electron accelerator (16-48 MeV)
IR beam is generated within the undulator placed in the optical cavity.

Tuning of the wavelength by adjusting the gap between two sets of magnets in the undulator.

At 40 MeV : access to the 800-2000 cm-1 band (Fingerprint region) with ~1 W of power.

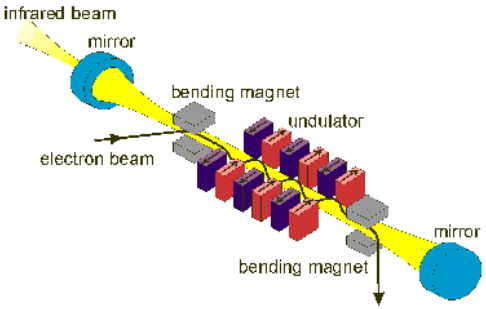

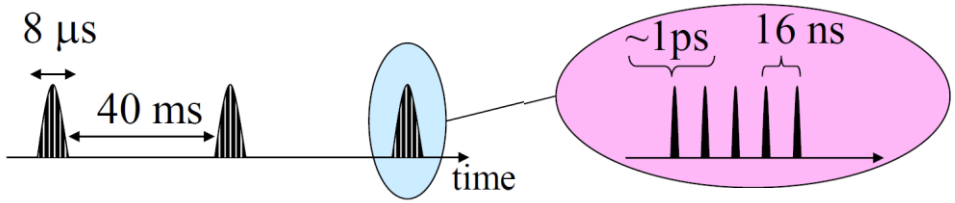

Photon sources for IRMPD

- Tunable lasers : table-top OPO-OPA lasers

  Based on the non-linear optical properties of crystal materials (such as KTP potassium titanyl phosphate)

  Repetition rate: 10 – 25 Hz, Power: ~10 mJ.

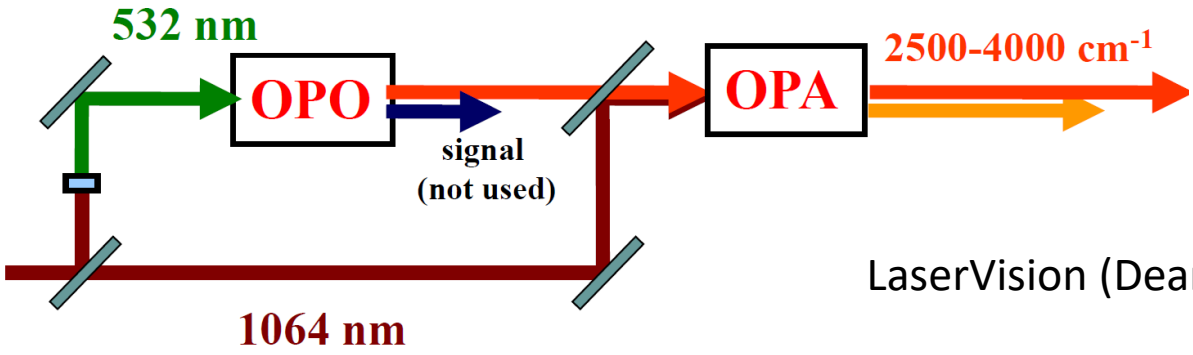

LaserVision (Dean Guyer)

Optical Parametric Oscillator Generates signal

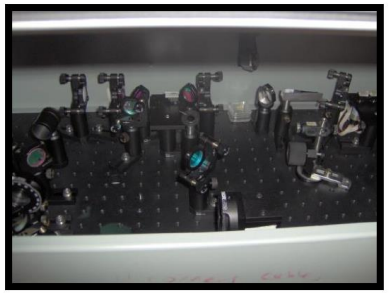

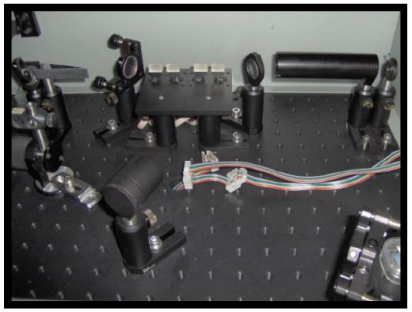

Optical Parametric Amplifier Boosts signal (single pass)

Photon sources for IRMPD

- CO_2 laser

- Electric discharge in a N_2 / CO_2 / He gas mixture
- High power conversion efficiency (up to 20%)
- High power (50 W or more can be purchased readily)
- Fixed wavelength (some are tunable) between 10.6 µm and 9.4 µm.

Principles of IRMPD

IVR : statistical redistribution of energy in several vibration modes of the molecule

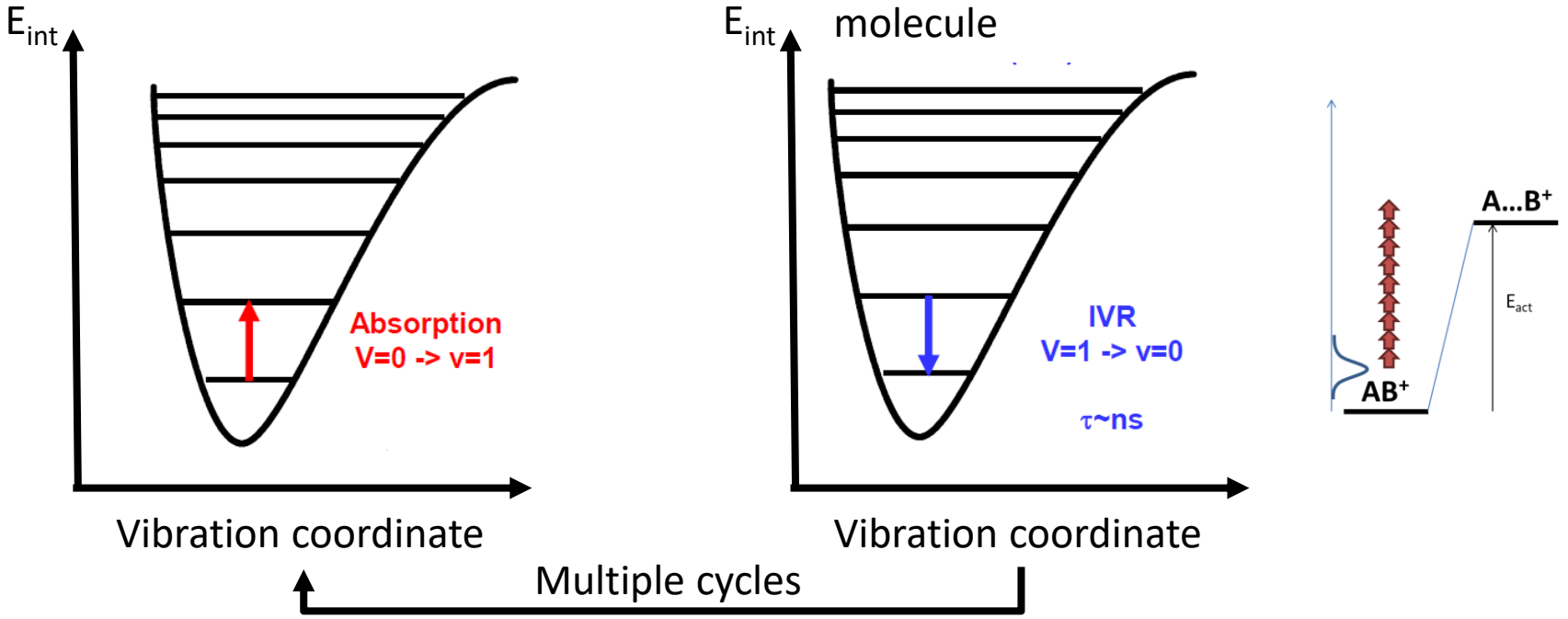

Referring to IRMPD : « This method employs an intense infrared laser to resonantly pump vibrational energy into the molecule in a **noncoherent** fashion, until it has sufficient energy to dissociate. »

R. C. Dunbar, D. T. Moore, J. Oomens, *J. Phys. Chem. A* **110**, 8316-8326 (2006)

Advantages of FT-ICR for IRMPD spectroscopy

- Multiphoton process can be inhibited by collisional relaxation.
  - In ion traps, relaxation occurs within 10 ms (P.M. Remes, G.L. Glish J. Am. Soc. Mass Spectrom. **20**, 1801 (2009)) which is shorter than the time between two OPO laser pulses or two FEL macropulses.
  - FT-ICR vacuum is thus better suited for IRMPD when a single pulse is not sufficient to accumulate sufficient amount of energy in an ion trap.
    - Many benefits for :
      - Large molecular systems (increased kinetic shift)
      - Strongly bound systems
      - Low intensity bands (but requires multiple passes and spectrum stiching).
    - Ion trap present the option of ion tagging as a subtitute for this limitation. But ion tagging can induce molecular structure shifts.

IRMPD spectroscopy in practice

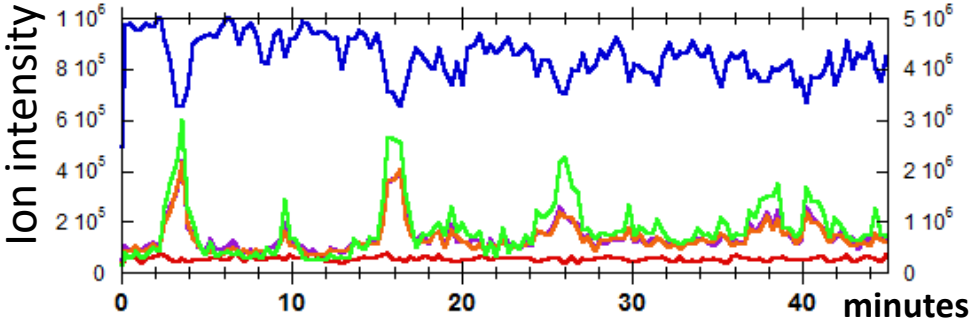

Spectrum recorded as an MS/MS chromatogram where each data point corresponds to one wavelength.
Synchronisation through instrument / laser TTL exchanges.

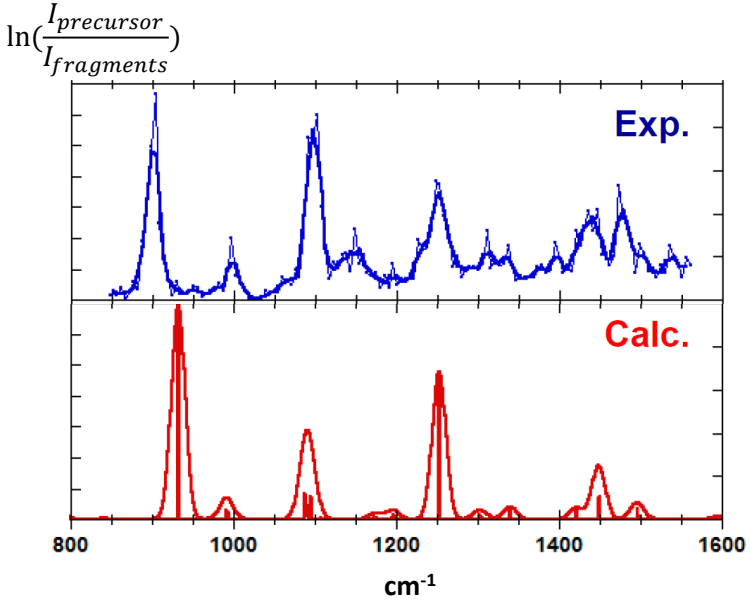

Comparison with calculated spectra

- Geometry optimization, mostly carried out with a standard basis set (6-31+G**)
  - Search for conformers with the lowest energy.
  - Harmonic bands are calculated from a frequency calculation and convoluted with a Gaussian profile (FWHM 10 or 20 cm^{-1})
- Scaling factors :
  - Multiple scaling factors have been proposed in the litterature depending on the method and basis set.
  - Issue is that most of the time the scaling factors differ between the fingerprint and harmonic regions (0.98 for fingerprint, 0.955 for X-H stretching region.

Scaling factors for IRMPD

- In 2017, we introduced the use of a linear scaling factor based on a series of 68 experimental values in the fingerprint region for which frequency assignment was structurally and spectrally unambiguous.
- The publication also introduces a measurement for similarity (similar to a Fisher test) which relies on the observed correlation for individual spectra.

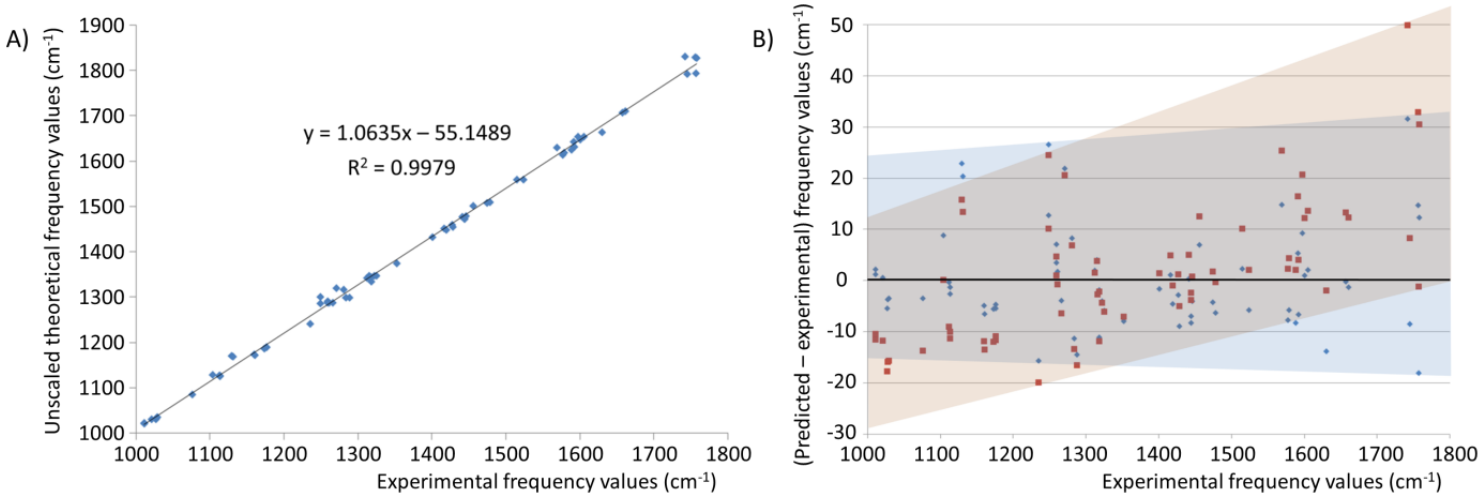

K. Madanakhrishna et al. Chem. Eur. J. **23**, 8414 (2017)

Improving OPO dissociation using CO_2 laser

- Low power of OPO laser can lead to situation in which radiative cooling exceeds resonant photoexcitation.
- CO_2 laser is synchronized with the OPO and irradiation time needs to be optimized for each system to set irradiation time just below the dissociation threshold.

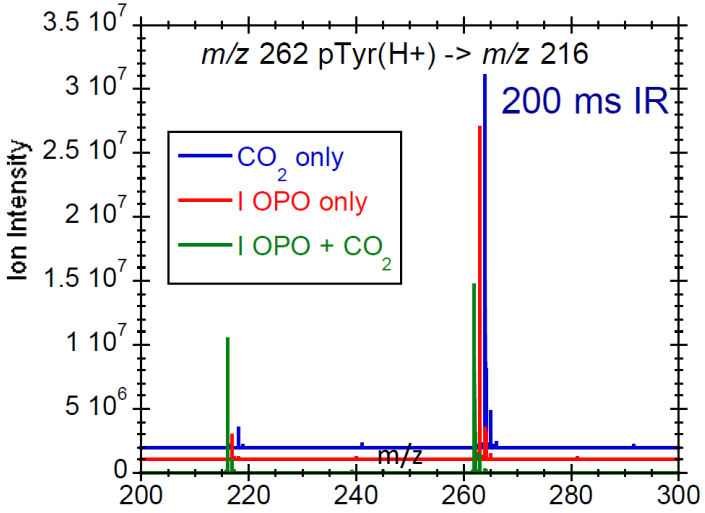

Phosphotyrosine+H⁺ : [pTyr+H]⁺

OPO, on resonance with an O-H band

OPO+CO_2: significant amplification

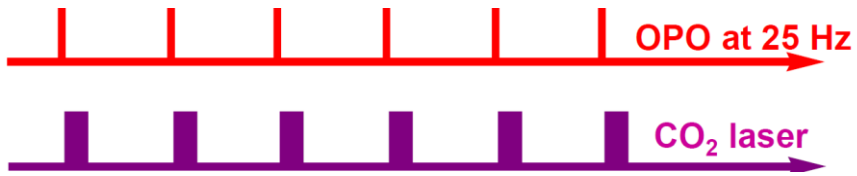

IRMPD at fixed wavelength

- Usually low intensity absorption bands in the fingerprint region at 943 cm^{-1}.
- High laser power (high photon density) compensates for the low intensity of the bands.

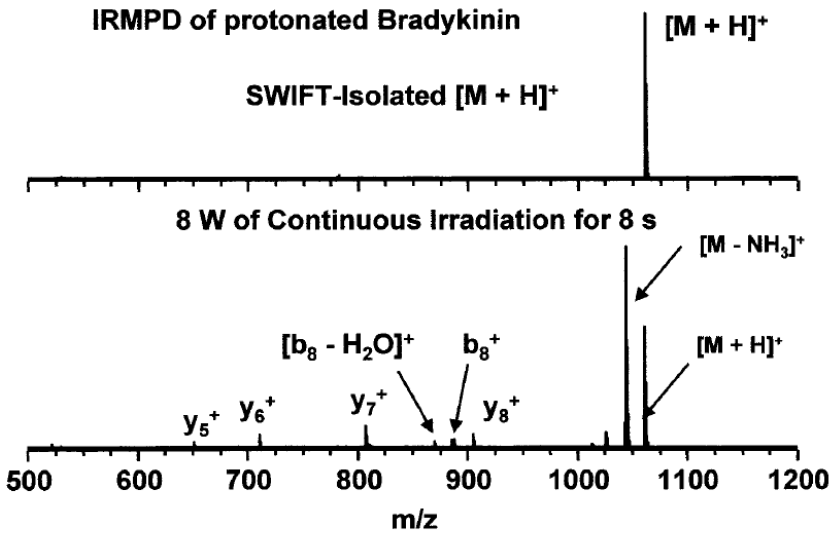

Figure 1. Infrared multiphoton dissociation (IRMPD) of protonated bradykinin, $[M+H]^+$. Protonated bradykinin was SWIFT-isolated (top) and irradiated with the IR laser for 8 s at 8 W (bottom).

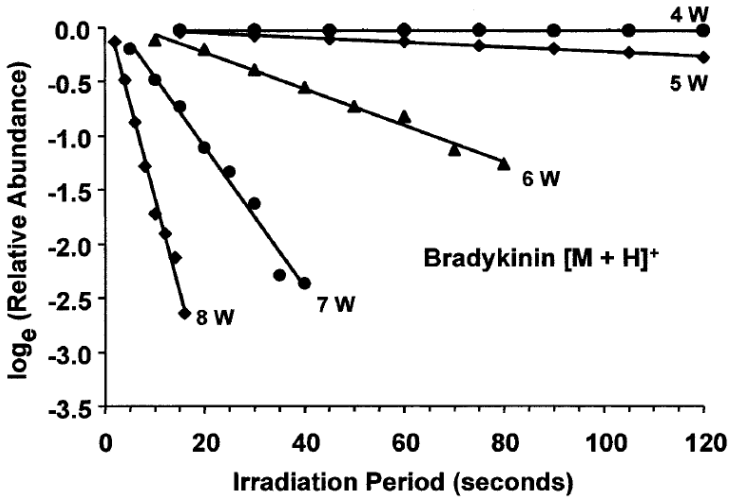

Figure 2. Plot of the natural logarithm of the relative abundance of protonated bradykinin, $[M+H]^+$, vs. time for unimolecular dissociation at each of five indicated laser powers. Note the highly linear behavior, showing that ions remain within the cross-section of the laser beam throughout the experiment.

M.A. Freitas et al. Rapid Comm. Mass Spectrom. **13**, 1639 (1999)

Resonant IRMPD with CO_2 laser

- Brodbelt and coworkers introduced the use of resonant IRMPD for phosphorylated peptides.

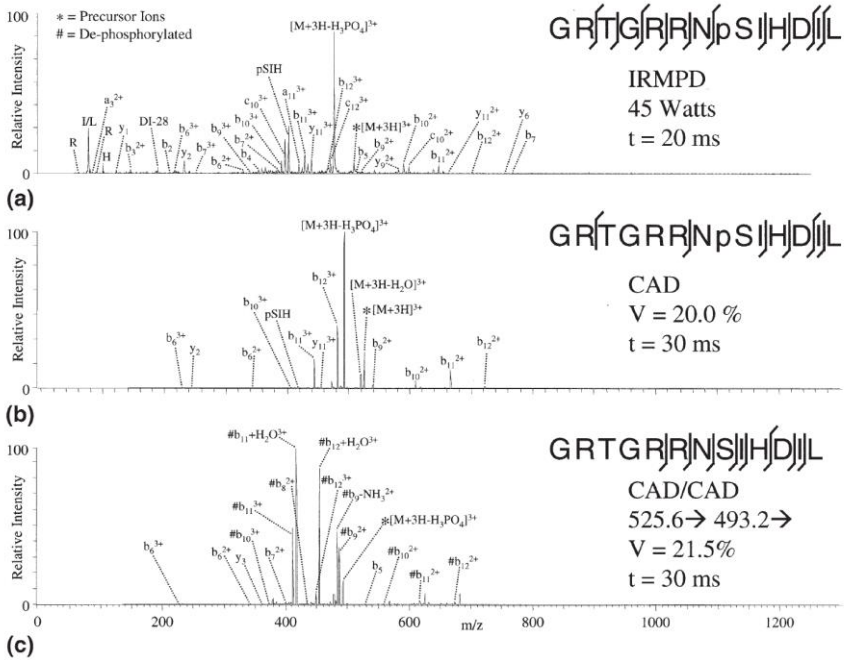

Figure 7. (a) IRMPD, (b) CAD MS^2, and (c) CAD MS^3 mass spectra of triply protonated GRT-GRRNpSIHDIL.

M.C. Crowe and J.S. Brodbelt, *J. Am. Soc. Mass Spectrom.* **15**, 1581 (2004)

Resonant IRMPD with CO_2 laser

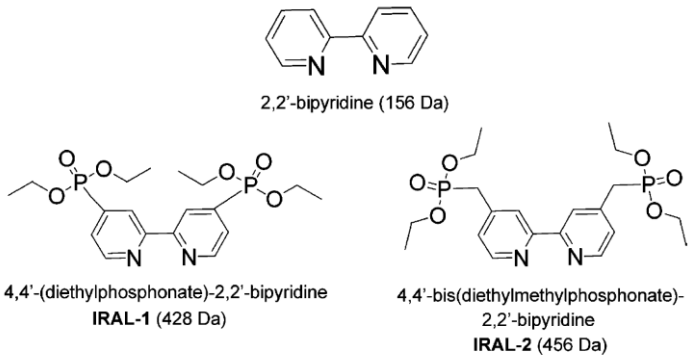

Figure 1. IR-active ligands based on the 2,2′-bipyridine skeleton synthesized and used in the study. Molecular weight is shown in parentheses.

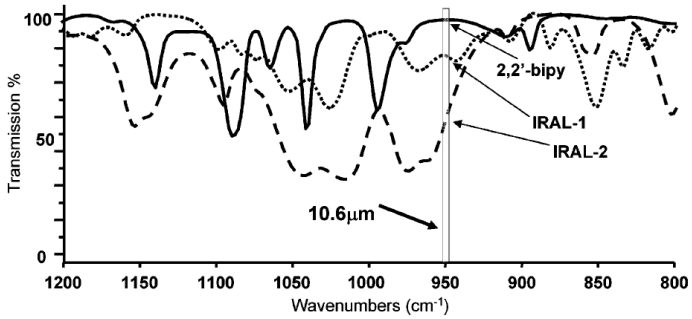

Figure 6. FTIR ATR spectra of the ligands used in the study, showing the enhanced absorption of the IR-active ligands, IRAL-1 and IRAL-2, at 10.6 μm as compared to 2,2′-bipyridine.

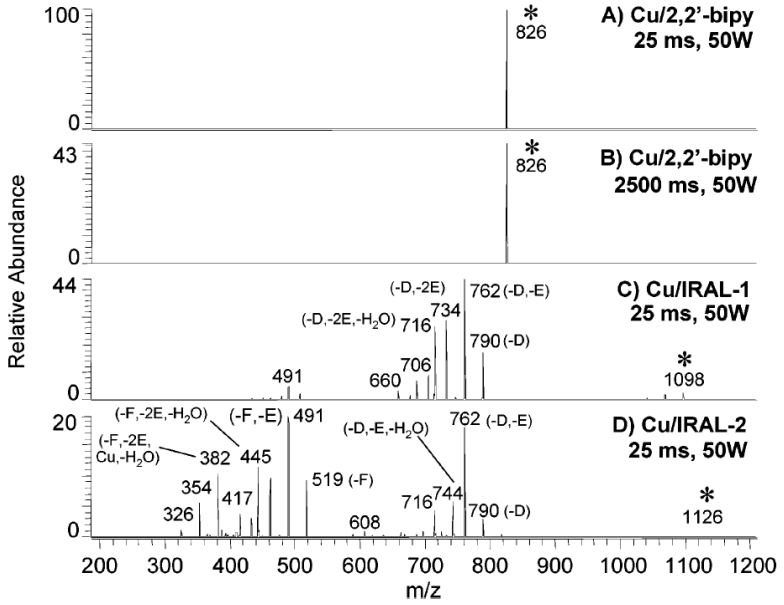

Figure 4. Irradiation of the $[Cu^{2+}(\text{neodiosmin} - H)\text{auxiliary ligand}]^+$ complexes containing different ligands: (A) $[Cu^{2+}(\text{neodiosmin} - H)2,2\text{-bipy}]^+$, 50 W for 25 ms; (B) $[Cu^{2+}(\text{neodiosmin} - H)2,2\text{-bipy}]^+$, 50 W for 2500 ms; (C) $[Cu^{2+}(\text{neodiosmin} - H)\text{IRAL-1}]^+$, 50 W for 25 ms; (D) $[Cu^{2+}(\text{neodiosmin} - H)\text{IRAL-2}]^+$, 50 W for 25 ms.

M. Pikulski et al. *Anal. Chem.* **78**, 8512 (2006)

Resonant excitation with tunable IR laser

- Peptide fragmentation has been abundantly studied using IRMPD spectroscopy.

b and a type ions have electrophilic and nucleophilic groups : cyclisation during the fragmentation process is an option.

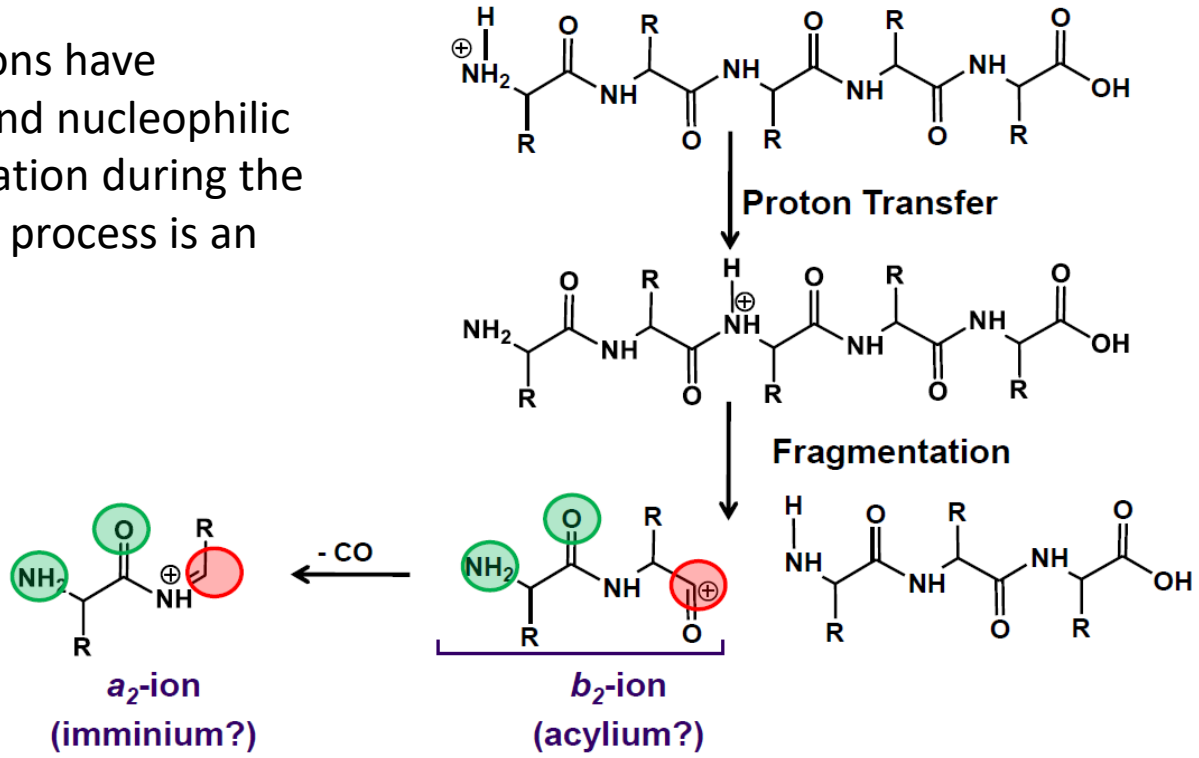

Peptide structures solved through tunable IRMPD

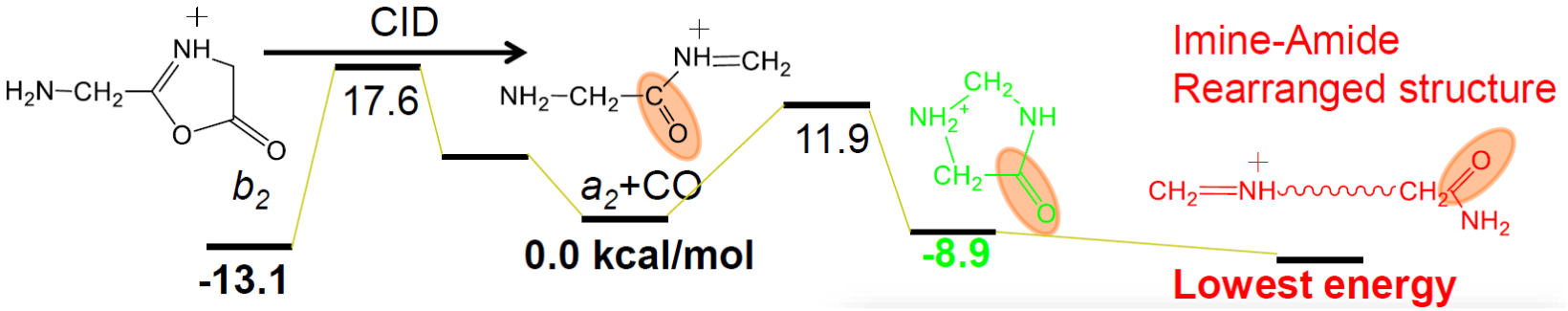

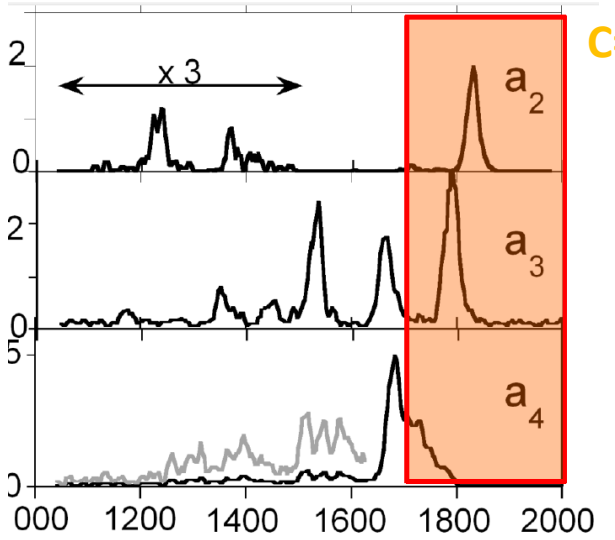

C=O stretch region

Oligoglycine a_2, a_3 and a_4 ions display strongly different C=O stretches.
Rearrangement of the an ions is kinetically controlled.

B. Bythell et al. J. Am. Chem. Soc **132**, 14766 (2010)

Peptide structures solved through IRMPD spectroscopy

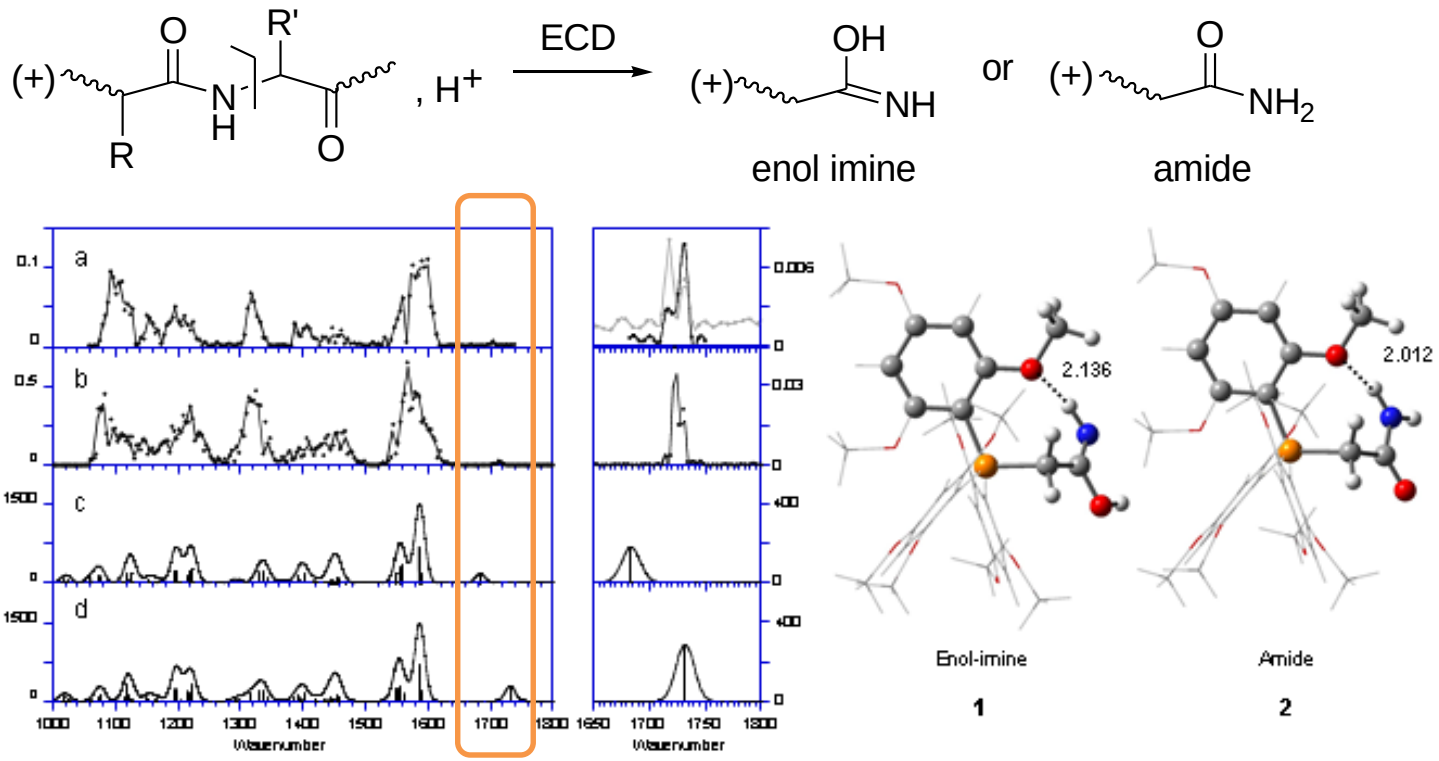

G. Frison et al. *J. Am. Chem. Soc.* ***130,*** 14916 (2008)

BIRD

- Radiative equilibrium between ions and cell walls.

Presure ~10^{-6}-10^{-8} mbar
t ~ 10s of seconds

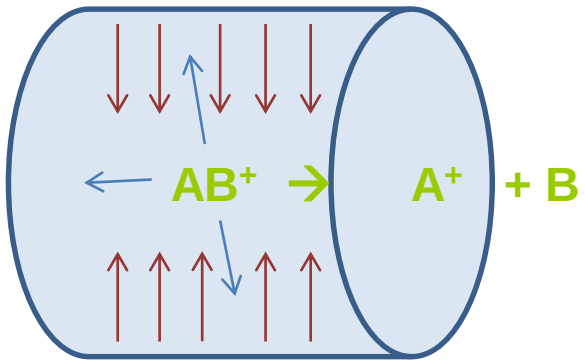

T_{walls}

Measurement of fragmentation kinetics at variable temperatures:

$$k(T) = A\, e^{-\frac{E_a}{RT}}$$

Access to kinetic parameters (A and E_a)

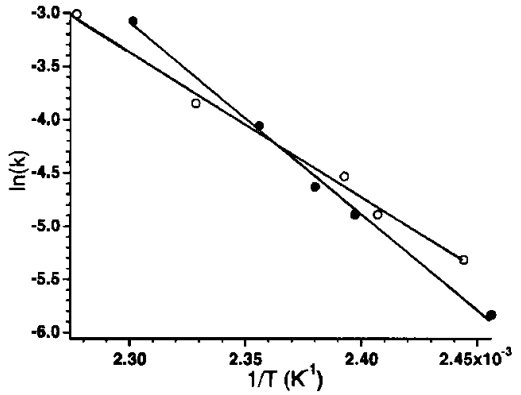

Figure 2. Arrhenius plot for dissociation of ubiquitin 5+ (○) (E_a = 1.2 eV; $A = 10^{12}$ s^{-1}) and 11+ (●) (E_a = 1.6 eV; $A = 10^{17}$ s^{-1}).

Application to a protein – ligand system

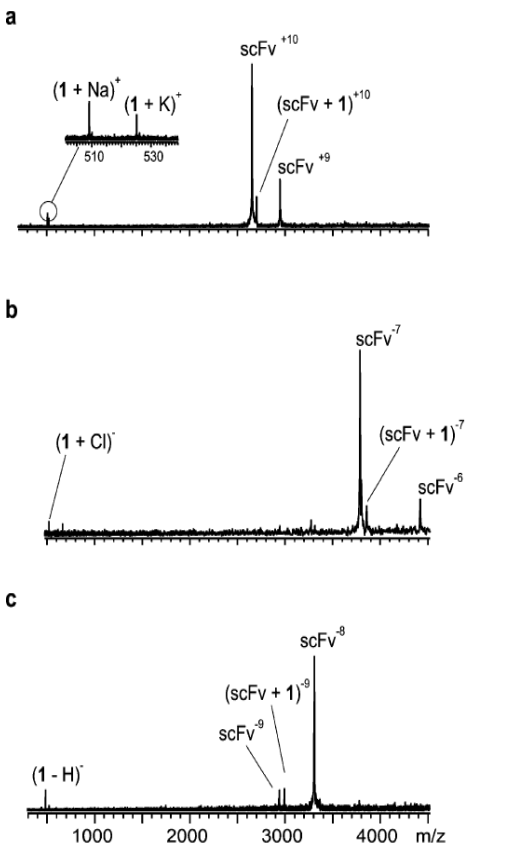

Figure 4. BIRD mass spectra obtained for protonated and deprotonated (scFv +**1**)$^{n+/-}$ ions (a) $n = +10$, 154 °C, 6 s; (b) $n = -8$, 147 °C, 5 s; (c) $n = -9$, 147 °C, 5 s.

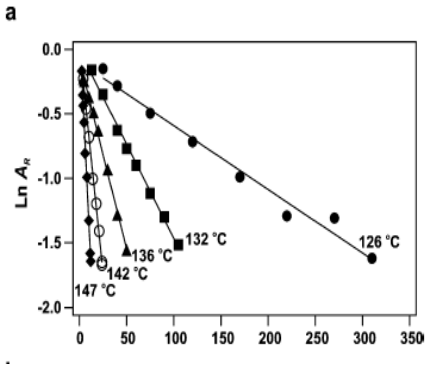

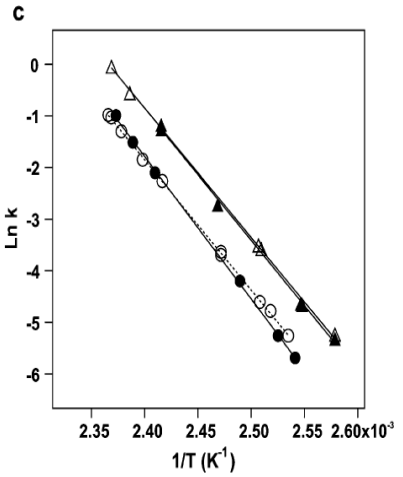

Figure 6. Arrhenius plots obtained for the loss of neutral L from the (P + L)$^{n+/-}$ ions: (a) L = **1**, P = scFv, +6 (◆), +7 (◇), +8 (△), +9 (▲), +10 (●), +11 (■), +12 (○), +13 (×), (b) L = **1**, P = scFv, −6 (□), −7 (▼), −8 (▽); (c) $n = +10$, L = **1**, P = scFv (●), L = **1**, P = His^{H101}Ala (○), L = **4**, P = scFv (▲), L = **4**, P = His^{H101}Ala (△).

E.N. Kitova et al, J. Am. Chem. Soc ***130****, 1214 (2008)*